

# Neutrino mixing sum rules and the Littlest Seesaw

---

Francesco Costa<sup>a</sup> Stephen F. King<sup>b</sup>

<sup>a</sup>*Institute for Theoretical Physics, Georg-August University Göttingen,  
Friedrich-Hund-Platz 1, Göttingen, D-37077 Germany*

<sup>b</sup>*School of Physics and Astronomy, University of Southampton,  
Southampton SO17 1BJ, United Kingdom*

*E-mail:* [francesco.costa@theorie.physik.uni-goettingen.de](mailto:francesco.costa@theorie.physik.uni-goettingen.de),  
[s.f.king@soton.ac.uk](mailto:s.f.king@soton.ac.uk)

ABSTRACT: In this work, we revisit neutrino mixing sum rules arising from discrete symmetries, and the class of Littlest Seesaw neutrino models. These theoretical models offer predictions for the leptonic CP phase and mixing angles, and correlations among them, which can be tested in forthcoming neutrino experiments. In particular we study the *solar* neutrino mixing sum rules, arising from charged lepton corrections to Tri-bimaximal (TB), Bi-maximal (BM), Golden Ratios (GRs) and Hexagonal (HEX) neutrino mixing, and *atmospheric* neutrino mixing sum rules, arising from preserving one of the columns of these types of mixing, for example the first or second column of the TB mixing matrix (TM1 or TM2), and confront them with an up-to-date global fit of the neutrino oscillation data. We show that some mixing sum rules, for example an *atmospheric* neutrino mixing sum rule arising from a version of neutrino Golden Ratio mixing (GRa1), are already excluded at  $3\sigma$ , and determine the remaining models allowed by the data. We also consider the highly predictive Littlest Seesaw models, which are a special case of tri-maximal mixing models (TM1), and discuss their prospects.

---

## Contents

<b>1</b>	<b>Introduction</b>	<b>1</b>
<b>2</b>	<b>Lepton mixing and symmetries</b>	<b>4</b>
<b>3</b>	<b>Solar sum rules</b>	<b>8</b>
<b>4</b>	<b>Atmospheric sum rules</b>	<b>12</b>
<b>5</b>	<b>Littlest Seesaw</b>	<b>16</b>
<b>6</b>	<b>Conclusions</b>	<b>23</b>

---

## 1 Introduction

Neutrino mass and mixing represents the first and so far only new physics beyond the Standard Model (SM) of particle physics. We know it must be new physics because its origin is unknown and it is not predicted by the SM. Independently of the whatever the new (or nu) SM is, we do know that the minimal paradigm involves three active neutrinos, the weak eigenstates  $\nu_e, \nu_\mu, \nu_\tau$  (the  $SU(2)_L$  partners to the left-handed charged lepton mass eigenstates) which are related to the three mass eigenstates  $m_{1,2,3}$  by a unitary PMNS mixing matrix [1].

The PMNS matrix is similar to the CKM matrix which describes quark mixing, but involves three independent leptonic mixing angles  $\theta_{23}, \theta_{13}, \theta_{12}$  (or  $s_{23} = \sin \theta_{23}$ ,  $s_{13} = \sin \theta_{13}$ ,  $s_{12} = \sin \theta_{12}$ ), one leptonic CP violating Dirac phase  $\delta$  which affects neutrino oscillations, and possibly two Majorana phases which do not enter into neutrino oscillation formulas. Furthermore neutrino oscillations only depend on the two mass squared differences  $\Delta m_{21}^2 = m_2^2 - m_1^2$ , which is constrained by data to be positive, and  $\Delta m_{31}^2 = m_3^2 - m_1^2$ , which current data allows to take a positive (normal) or negative (inverted) value. In 1998, the angle  $\theta_{23}$  was first measured to be roughly  $45^\circ$  (consistent with equal bi-maximal  $\nu_\mu - \nu_\tau$  mixing) by atmospheric neutrino oscillations, while  $\theta_{12}$  was determined to be roughly  $35^\circ$  (consistent with equal tri-maximal  $\nu_e - \nu_\mu - \nu_\tau$  mixing) in 2002 by solar neutrino oscillation experiments, while  $\theta_{13}$  was first accurately found to be  $8.5^\circ$  in 2012 by reactor oscillation experiments.

Various simple ansatzes for the PMNS matrix were proposed, the most simple ones involving a zero reactor angle and bimaximal atmospheric mixing,  $s_{13} = 0$  and  $s_{23} = c_{23} = 1/\sqrt{2}$ , leading to a PMNS matrix of the form,

$$U_0 = \begin{pmatrix} c_{12} & s_{12} & 0 \\ -\frac{s_{12}}{\sqrt{2}} & \frac{c_{12}}{\sqrt{2}} & \frac{1}{\sqrt{2}} \\ \frac{s_{12}}{\sqrt{2}} & -\frac{c_{12}}{\sqrt{2}} & \frac{1}{\sqrt{2}} \end{pmatrix}, \quad (1.1)$$

where the zero subscript reminds us that this form has  $\theta_{13} = 0$  (and  $\theta_{23} = 45^\circ$ ).

For golden ratio (GRa) mixing [2], the solar angle is given by  $\tan \theta_{12} = 1/\phi$ , where  $\phi = (1 + \sqrt{5})/2$  is the golden ratio which implies  $\theta_{12} = 31.7^\circ$ . There are two alternative versions where  $\cos \theta_{12} = \phi/2$  and  $\theta_{12} = 36^\circ$  [3] which we refer to as GRb mixing, and GRc where  $\cos \theta_{12} = \phi/\sqrt{3}$  and  $\theta_{12} \approx 20.9^\circ$ .

For bimaximal (BM) mixing (see e.g. [4–6] and references therein), we insert  $s_{12} = c_{12} = 1/\sqrt{2}$  ( $\theta_{12} = 45^\circ$ ) into Eq. (1.1),

$$U_{\text{BM}} = \begin{pmatrix} \frac{1}{\sqrt{2}} & \frac{1}{\sqrt{2}} & 0 \\ -\frac{1}{2} & \frac{1}{2} & \frac{1}{\sqrt{2}} \\ \frac{1}{2} & -\frac{1}{2} & \frac{1}{\sqrt{2}} \end{pmatrix}. \quad (1.2)$$

For tri-bimaximal (TB) mixing [7], alternatively we use  $s_{12} = 1/\sqrt{3}$ ,  $c_{12} = \sqrt{2/3}$  ( $\theta_{12} = 35.26^\circ$ ) in Eq. (1.1),

$$U_{\text{TB}} = \begin{pmatrix} \sqrt{\frac{2}{3}} & \frac{1}{\sqrt{3}} & 0 \\ -\frac{1}{\sqrt{6}} & \frac{1}{\sqrt{3}} & \frac{1}{\sqrt{2}} \\ \frac{1}{\sqrt{6}} & -\frac{1}{\sqrt{3}} & \frac{1}{\sqrt{2}} \end{pmatrix}. \quad (1.3)$$

Finally another pattern studied in the literature with  $\theta_{13} = 0$  (and  $\theta_{23} = 45^\circ$ ) is the hexagonal mixing (HEX) where  $\theta_{12} = \pi/6$ .

These proposals are typically by finite discrete symmetries such as  $A_4, S_4, S_5$  (for a review see e.g. [8]). After the reactor angle was measured, which excluded all these ansatze, there were various proposals to rescue them and hence to maintain the notion of predictivity of the leptonic mixing parameters, in particular the Dirac CP phase  $\delta$ , which is not directly measured so far and remains poorly determined even indirectly. Two approaches have been developed, in which some finite symmetry (typically a subgroup of  $A_4, S_4, S_5$ ) can enforce a particular structure of the PMNS matrix consistent with a non-zero reactor angle, leading to *solar* and *atmospheric* sum rules, as we now discuss.

The first approach, which leads to *solar* sum rules, is to assume that the above patterns of mixing still apply to the neutrino sector, but receive charged lepton mixing corrections due to the PMNS matrix being the product of two unitary matrices, which in our convention is written as  $V_{eL} V_{\nu L}^\dagger$ , where  $V_{\nu L}^\dagger$  is assumed to take the BM, TB or GR form, while  $V_{eL}$  differs from the unit matrix. If  $V_{eL}$  involves negligible 13 charged lepton mixing, then it is possible to generate a non-zero 13 PMNS mixing angle, while leading to correlations amongst the physical PMNS parameters, known as *solar* mixing sum rules [9–12]. This scenario may be enforced by a subgroup of  $A_4, S_4, S_5$  which enforces the  $V_\nu$  structure [8] while allowing charged lepton corrections.

In the second approach, which leads to *atmospheric* sum rules, it is assumed that the physical PMNS mixing matrix takes the BM, TB or GR form but only in its first or second column, while the third column necessarily departs from these structures due to the non-zero 13 angle. Such patterns again lead to correlations amongst the physical PMNS parameters, known as *atmospheric* mixing sum rules. This scenario may be enforced by

a subgroup of  $A_4, S_4, S_5$  which enforces the one column  $V_\nu$  structure [8] while forbidding charged lepton corrections.

Apart from the large lepton mixing angles, another puzzle is the extreme lightness of neutrino masses. Although the type I seesaw mechanism can qualitatively explain the smallness of neutrino masses through the heavy right-handed neutrinos (RHNs), if one doesn't make other assumptions, it contains too many parameters to make any particular predictions for neutrino mass and mixing. The sequential dominance (SD) [13, 14] of right-handed neutrinos proposes that the mass spectrum of heavy Majorana neutrinos is strongly hierarchical, i.e.  $M_{\text{atm}} \ll M_{\text{sol}} \ll M_{\text{dec}}$ , where the lightest RHN with mass  $M_{\text{atm}}$  is responsible for the atmospheric neutrino mass, that with mass  $M_{\text{sol}}$  gives the solar neutrino mass, and a third largely decoupled RHN gives a suppressed lightest neutrino mass. It leads to an effective two right-handed neutrino (2RHN) model [15, 16] with a natural explanation for the physical neutrino mass hierarchy, with normal ordering and the lightest neutrino being approximately massless,  $m_1 = 0$ .

A very predictive minimal seesaw model with two right-handed neutrinos and one texture zero is the so-called constrained sequential dominance (CSD) model [9, 17–25]. The CSD( $n$ ) scheme, also known as the Littlest Seesaw, assumes that the two columns of the Dirac neutrino mass matrix are proportional to  $(0, 1, -1)$  and  $(1, n, 2-n)$  or  $(1, 2-n, n)$  respectively in the RHN diagonal basis (or equivalently  $(0, 1, 1)$  and  $(1, n, n-2)$  or  $(1, n-2, n)$ ) where the parameter  $n$  was initially assumed to be a positive integer, but in general may be a real number. For example the CSD(3) (also called Littlest Seesaw model) [18–22], CSD(4) models [23, 24] and CSD(2.5) [26] can give rise to phenomenologically viable predictions for lepton mixing parameters and the two neutrino mass squared differences  $\Delta m_{21}^2$  and  $\Delta m_{31}^2$ , corresponding to special constrained cases of lepton mixing which preserve the first column of the TB mixing matrix, namely TM1 and hence satisfy *atmospheric* mixing sum rules. As was observed, modular symmetry remarkably suggests CSD( $1 + \sqrt{6}$ )  $\approx$  CSD(3.45) [27–30].

In this paper we shall revisit neutrino *solar* and *atmospheric* mixing sum rules arising from discrete symmetries, and also discuss the class of Littlest Seesaw models. These theoretical models offer predictions for the leptonic CP phase and mixing angles, and correlations among them, which can be tested in forthcoming neutrino experiments. In particular we study the *solar* neutrino mixing sum rules, arising from charged lepton corrections to TB, BM and GR neutrino mixing, and *atmospheric* neutrino mixing sum rules, arising from preserving one of the columns of these types of mixing, for example the first or second column of the TB mixing matrix (TM1 or TM2), and confront them with an up-to-date global fit of the neutrino oscillation data. We show that some mixing sum rules, for example all the *atmospheric* neutrino mixing sum rule arising from a Golden Ratio mixings are already excluded at  $3\sigma$  a part from GRa2, and determine the remaining models allowed by the data. We also consider the highly predictive Littlest Seesaw models, which are a special case of tri-maximal mixing models (TM1), and discuss their prospects.

The layout of the remainder of the paper is as follows. In Chapter 2 we introduce the notation for the PMNS matrix and discuss the symmetries of the leptonic Lagrangian. In Chapter 3 and 4 we introduce the *atmospheric* and *solar* sum rules for the different

models we are studying and confront them with the up-to-date neutrino data global fit. We proceed in Chapter 5 discussing the CDS and the Littlest Seesaw model, showing its high predictivity and the viable parameter space given the experimental data and its fit. Finally we conclude in Chapter 6.

## 2 Lepton mixing and symmetries

The mixing matrix in the lepton sector, the PMNS matrix  $U_{\text{PMNS}}$ , is defined as the matrix which appears in the electroweak coupling to the  $W$  bosons expressed in terms of lepton mass eigenstates. With the mass matrices of charged leptons  $M_e$  and neutrinos  $m_{LL}^\nu$  written as<sup>1</sup>

$$L = -\bar{e}_L M_e e_R - \frac{1}{2} \bar{\nu}_L M^\nu \nu_L^c + H.c. , \quad (2.1)$$

and performing the transformation from flavour to mass basis by

$$V_{e_L} M_e V_{e_R}^\dagger = \text{diag}(m_e, m_\mu, m_\tau), \quad V_{\nu_L} M^\nu V_{\nu_L}^T = \text{diag}(m_1, m_2, m_3), \quad (2.2)$$

the PMNS matrix is given by

$$U_{\text{PMNS}} = V_{e_L} V_{\nu_L}^\dagger . \quad (2.3)$$

Here it is assumed implicitly that unphysical phases are removed by field redefinitions, and  $U_{\text{PMNS}}$  contains one Dirac phase and two Majorana phases. The latter are physical only in the case of Majorana neutrinos, for Dirac neutrinos the two Majorana phases can be absorbed as well.

According to the above discussion, the neutrino mass and flavour bases are misaligned by the PMNS matrix as follows,

$$\begin{pmatrix} \nu_e \\ \nu_\mu \\ \nu_\tau \end{pmatrix} = \begin{pmatrix} U_{e1} & U_{e2} & U_{e3} \\ U_{\mu1} & U_{\mu2} & U_{\mu3} \\ U_{\tau1} & U_{\tau2} & U_{\tau3} \end{pmatrix} \begin{pmatrix} \nu_1 \\ \nu_2 \\ \nu_3 \end{pmatrix} \equiv U_{\text{PMNS}} \begin{pmatrix} \nu_1 \\ \nu_2 \\ \nu_3 \end{pmatrix}, \quad (2.4)$$

where  $\nu_e, \nu_\mu, \nu_\tau$  are the  $SU(2)_L$  partners to the left-handed charged lepton mass eigenstates and  $\nu_{1,2,3}$  are the neutrinos in their mass basis. Following the standard convention we can describe  $U_{\text{PMNS}}$  in terms of three angles, one CP violation phase and two Majorana phases

$$U_{\text{PMNS}} = \begin{pmatrix} 1 & 0 & 0 \\ 0 & c_{23} & s_{23} \\ 0 & -s_{23} & c_{23} \end{pmatrix} \begin{pmatrix} c_{13} & 0 & s_{13} e^{-i\delta} \\ 0 & 1 & 0 \\ -s_{13} e^{i\delta} & 0 & c_{13} \end{pmatrix} \begin{pmatrix} c_{12} & s_{12} & 0 \\ -s_{12} & c_{12} & 0 \\ 0 & 0 & 1 \end{pmatrix} P, \quad (2.5)$$

---

<sup>1</sup>Although we have chosen to write a Majorana mass matrix, all relations in the following are independent of the Dirac or Majorana nature of neutrino masses.

$$= \begin{pmatrix} c_{12}c_{13} & s_{12}c_{13} & s_{13}e^{-i\delta} \\ -s_{12}c_{23} - c_{12}s_{13}s_{23}e^{i\delta} & c_{12}c_{23} - s_{12}s_{13}s_{23}e^{i\delta} & c_{13}s_{23} \\ s_{12}s_{23} - c_{12}s_{13}c_{23}e^{i\delta} & -c_{12}s_{23} - s_{12}s_{13}c_{23}e^{i\delta} & c_{13}c_{23} \end{pmatrix} P, \quad (2.6)$$

where  $P$  contains the Majorana phases

$$P = \text{diag} \left( 1, e^{i\alpha_{21}/2}, e^{i\alpha_{31}/2} \right), \quad (2.7)$$

The current  $3\sigma$  parameters intervals coming from the global fit of the neutrino oscillation data by the `nuFIT` collaboration [31] are

$$\theta_{12} = [31.31^\circ, 35.74^\circ], \quad \theta_{23} = [39.6^\circ, 51.9^\circ], \quad \theta_{13} = [8.19^\circ, 8.89^\circ], \quad (2.8)$$

$$\delta = [0^\circ, 44^\circ] \quad \& \quad [108^\circ, 360^\circ], \quad \frac{\Delta_{21}^2}{10^{-5}\text{eV}^2} = [6.82, 8.03], \quad \frac{\Delta_{3l}^2}{10^{-3}\text{eV}^2} = [2.428, 2.597]. \quad (2.9)$$

The PMNS matrix reads

$$|U|_{3\sigma}^{\text{w/o SK-atm}} = \begin{pmatrix} 0.803 \rightarrow 0.845 & 0.514 \rightarrow 0.578 & 0.142 \rightarrow 0.155 \\ 0.233 \rightarrow 0.505 & 0.460 \rightarrow 0.693 & 0.630 \rightarrow 0.779 \\ 0.262 \rightarrow 0.525 & 0.473 \rightarrow 0.702 & 0.610 \rightarrow 0.762 \end{pmatrix}. \quad (2.10)$$

These results are obtained considering normal ordering, which is the current best fit, and without including the Super-Kamiokande (SK) data. Simple mixing patters such TB, BM or GR could explain the first neutrino oscillation data. These patterns can be enforced via symmetries of the mass matrices. Let us take a basis where the charged lepton  $M_e$  mass matrix is diagonal and we notice that for 3 generations we have that  $Z_3^T$  is a symmetry of the Lagrangian

$$T^\dagger \left( M_e^\dagger M_e \right) T = M_e^\dagger M_e, \quad (2.11)$$

where  $T = \text{diag} (1, \omega^2, \omega)$  and  $\omega = e^{i2\pi/3}$ . The light Majorana neutrino mass matrix is invariant under the Klein symmetry:  $Z_2^U \times Z_2^S$ . This can be seen taking the diagonal neutrino mass matrix and performing the transformations

$$M^\nu = S^T M^\nu S, \quad M^\nu = U^T M^\nu U, \quad (2.12)$$

and  $M^\nu$  is left invariant with

$$\begin{aligned} S &= U_{\text{PMNS}}^* \text{diag}(+1, -1, -1) U_{\text{PMNS}}^T \\ U &= U_{\text{PMNS}}^* \text{diag}(-1, +1, -1) U_{\text{PMNS}}^T \end{aligned} \quad (2.13)$$

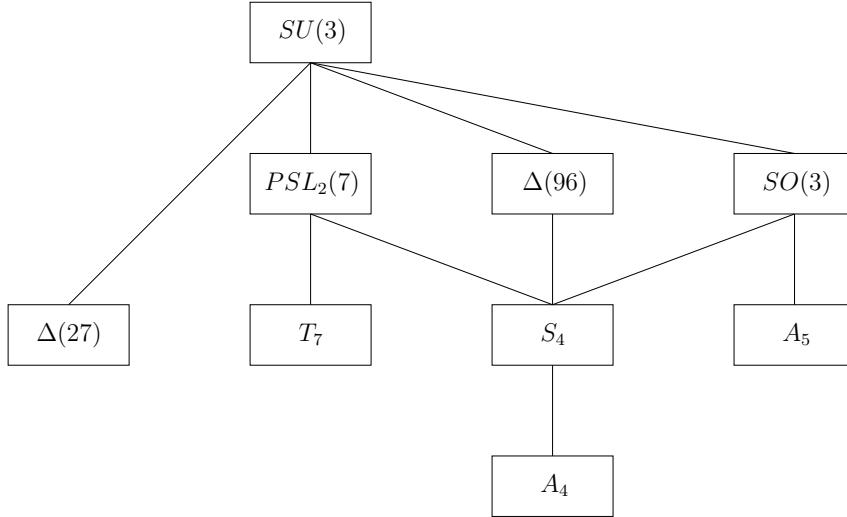


**Figure 1:** Subgroups of  $SU(3)$  with triplet representations. The smaller of two groups connected in the graph is a subset of the other. Figure from [8].

## Tri-bimaximal mixing

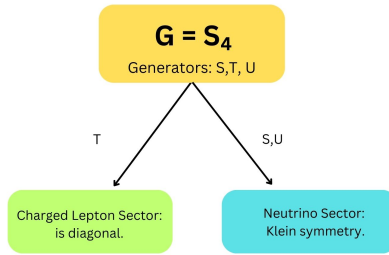


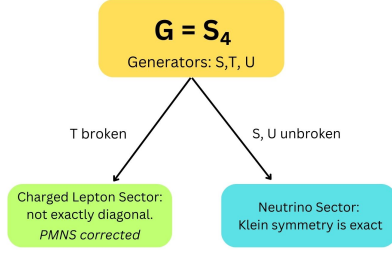
**Figure 2:** A schematic diagram that illustrates the way that the two subgroups  $Z_2^U \times Z_2^S$  and  $Z_3^T$  of a finite group work in the charged lepton and neutrino sectors in order to enforce a particular pattern of PMNS mixing. In this example, the group  $S_4$  leads to TB mixing.

where this result follows from the fact that, in the charged lepton mass eigenstate basis, the neutrino mass matrix is diagonalised by  $U_{\text{PMNS}}$  as in Eq. (2.2), where any two diagonal matrices commute. Then Eq. (2.13) shows that the matrices  $S, U$  are both diagonalised by the same matrix  $U_{\text{PMNS}}$  that also diagonalises the neutrino mass matrix. Given this result, we can always find the two matrices  $S, U$  for any PMNS mixing matrix, and hence the Klein symmetry is present for any choice of the PMNS mixing. However not all Klein symmetries may be identified with finite groups of low order.

This description is meaningful if the charged leptons are diagonal ( $T$  is conserved) or approximately diagonal ( $T$  is softly broken). We are therefore interested in finite groups that are superset of  $Z_2^U \times Z_2^S$  and  $Z_3^T$  and have a triplet representation. Groups of low order that satisfy these constraints are given in Figure 1.

One simple example is the group  $G = S_4$ , of order 24, which is the group of permutation of 4 objects. The generators follow the presentation rules [8]

## Solar sum rules



## Atmospheric sum rules

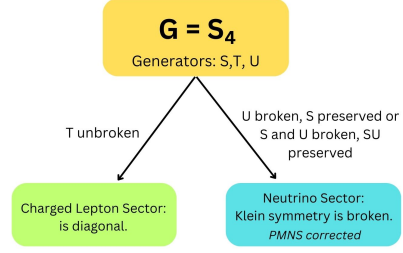


**Figure 3:** In order to generate a non-zero (13) PMNS element, one or more of the generators  $S, T, U$  must be broken. In the left panel we depict  $T$  breaking leading to charged lepton mixing corrections and possible *solar* sum rules. In the right panel,  $U$  is broken, while either  $S$  or  $SU$  is preserved leading to neutrino mixing corrections and *atmospheric* sum rules.

$$S^2 = T^3 = (ST)^3 = U^2 = (TU)^2 = (SU)^2 = (STU)^4 = \mathbf{1}, \quad (2.14)$$

The two possible  $S_4$  triplet irreducible representations with a standard choice of basis [32], gives the generators explicit expression

$$S = \frac{1}{3} \begin{pmatrix} -1 & 2 & 2 \\ 2 & -1 & 2 \\ 2 & 2 & -1 \end{pmatrix}, \quad T = \begin{pmatrix} 1 & 0 & 0 \\ 0 & \omega^2 & 0 \\ 0 & 0 & \omega \end{pmatrix}, \quad U = \mp \begin{pmatrix} 1 & 0 & 0 \\ 0 & 0 & 1 \\ 0 & 1 & 0 \end{pmatrix}, \quad (2.15)$$

where again  $\omega = e^{i2\pi/3}$  and the sign of the  $U$  matrix corresponds to the two different triplet representation. The group  $S_4$  predicts a TB mixing [7], see Figure ???. This can be checked by the fact that  $S$  and  $U$  are diagonalised by  $U_{\text{TB}}$ , see Equations (2.13). Another commonly used group is  $A_4$ , which has two generators  $S$  and  $U$  that follow the same presentation rules as in Equation (2.14) and in a standard basis [33], the generators have the same form as in Equation (2.15).

In order to explain the experimental results  $G$  needs to be broken and generate a non-zero (13) PMNS element. This will lead to corrections to the leading order PMNS predictions from the discrete group  $G$ . In Figure 3 we illustrate two possible direction we can proceed to do that. The first one is to break the  $T$  generator while the Klein symmetry in the neutrino sector is exact (left hand side). This means that the charged lepton matrix is approximately diagonal. In the mass basis we will have then a correction to the neutrino mixing matrix by a unitary matrix  $V_e$  and the PMNS is now  $U_{\text{PMNS}} = V_e^\dagger V_\nu$ . Applying this to a group  $G$  will lead to *solar* sum rules. The second direction is to preserve  $Z_3^T$  but breaking  $Z_2^U$  while keeping either  $Z_2^{SU}$  or  $Z_2^S$  unbroken (right hand side). This leads to corrections to the prediction of  $G$  within the neutrino mixing and to *atmospheric* sum rules. It is convenient to introduce small parameters that can simplify the sum rules expressions and help us understand their physical behaviour since both in



*solar* and *atmospheric* sum rules we implement a small deviation from the prediction of the exact finite discrete symmetries. We can consider the deviation parameters  $s, r, a$  [34]

$$\sin \theta_{12} \equiv \frac{1+s}{\sqrt{3}}, \quad \sin \theta_{13} \equiv \frac{r}{\sqrt{2}}, \quad \sin \theta_{23} \equiv \frac{1+a}{\sqrt{2}}, \quad (2.16)$$

that highlight the differences from TB mixing. Given the latest fit the  $3\sigma$  allowed range for the solar, reactor and atmospheric deviation are respectively

$$\begin{aligned} -0.0999 < s < 0.0117, \\ 0.20146 < r < 0.21855, \\ -0.0985 < a < 0.1129. \end{aligned} \quad (2.17)$$

This shows that the reactor angle differs from zero significantly ( $r \neq 0$ ), but the solar and atmospheric angles remain consistent with TB mixing ( $s = a = 0$ ) at  $3\sigma$ . From a theoretical point of view, one of the goals of the neutrino experiments would be to exclude the TB prediction  $s = a = 0$  [35], which is so far still allowed at  $3\sigma$ .

### 3 Solar sum rules

The first possibility to generate a non-zero reactor angle, whilst maintaining some of the predictivity of the original mixing patterns, is to allow the the charged lepton sector to give a mixing correction to the leading order mixing matrix  $U_\nu$ . This will lead to the so-called *solar* sum rules, that are relations between the parameters that can be tested. This operation is equivalent to considering the  $T$  generator of the  $S_4$  symmetry which enforces the charged lepton mass matrix to be diagonal (in our basis) to be broken.

When the  $T$  generator is broken, the charged lepton matrix is not exactly diagonal and it will give a correction to the PMNS matrix predicted by the symmetry group  $G$ . For example for the  $S_4$ ,  $U_{\text{PMNS}}$  is not exactly  $U_{\text{TB}}$  but it receives a correction that we will compute. The fact that  $S$  and  $U$  are preserved leads to a set of correlations among the physical parameters, the *solar* sum rules which are the prediction of the model. For the *solar* sum rules we can obtain a prediction for  $\cos \delta$  as we shall now show.

For example consider the case of TB neutrino mixing with the charged lepton mixing corrections involving only (1,2) mixing, so that the PMNS matrix in Eq. 2.3 is given by,

$$U_{\text{PMNS}} = \begin{pmatrix} c_{12}^e & s_{12}^e e^{-i\delta_{12}^e} & 0 \\ -s_{12}^e e^{i\delta_{12}^e} & c_{12}^e & 0 \\ 0 & 0 & 1 \end{pmatrix} \begin{pmatrix} \sqrt{\frac{2}{3}} & \frac{1}{\sqrt{3}} & 0 \\ -\frac{1}{\sqrt{6}} & \frac{1}{\sqrt{3}} & \frac{1}{\sqrt{2}} \\ \frac{1}{\sqrt{6}} & -\frac{1}{\sqrt{3}} & \frac{1}{\sqrt{2}} \end{pmatrix} = \begin{pmatrix} \dots & \dots & \frac{s_{12}^e}{\sqrt{2}} e^{-i\delta_{12}^e} \\ \dots & \dots & \frac{c_{12}^e}{\sqrt{2}} \\ \frac{1}{\sqrt{6}} & -\frac{1}{\sqrt{3}} & \frac{1}{\sqrt{2}} \end{pmatrix} \quad (3.1)$$

The elements of the PMNS matrix are clearly related by [12, 37]

$$\frac{|U_{\tau 1}|}{|U_{\tau 2}|} = \frac{s_{12}^\nu}{c_{12}^\nu} = t_{12}^\nu = \frac{1}{\sqrt{2}}. \quad (3.2)$$

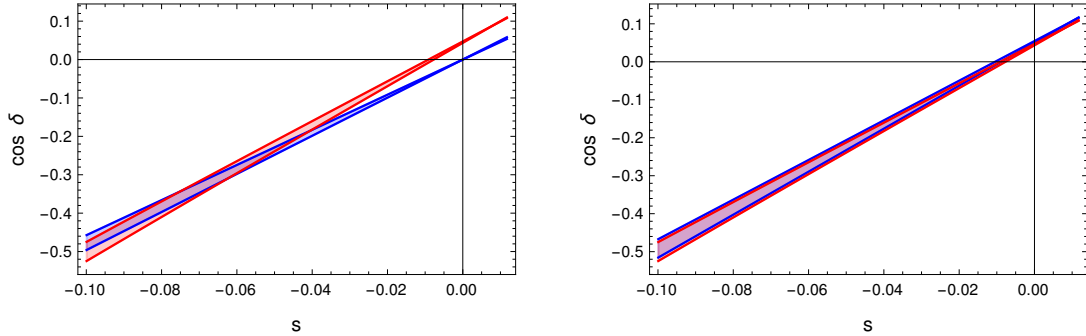


**Figure 4:** *Solar* mixing sum rule predictions for TB neutrino mixing. In the both panels the red band is the allowed region of the exact TB *solar* sum rules using the  $3\sigma$  range of  $r$  (i.e. the deviation of  $\sin \theta_{13}$ ) and it is plotted in the  $3\sigma$  range of  $s$  (i.e. the deviation of  $\sin \theta_{23}$  from the TB value) and using the best fit value for  $a = 0.071$ . The blue band is given by the linearised sum rule. In the right panel the blue band is the second order expansion sum rule prediction, it matches the exact sum rule.

This relation is easy to understand if we consider only one charged lepton angle to be non-zero,  $\theta_{12}^e$  then the third row of the PMS matrix in Eq. 3.1 is unchanged, so the elements  $U_{\tau i}$  may be identified with the corresponding elements in the uncorrected mixing matrix in Eq.1.1. Interestingly, the above relation still holds even if both  $\theta_{12}^e$  and  $\theta_{23}^e$  are non-zero. However it fails if  $\theta_{13}^e \neq 0$  [36].

The above relation in Eq.3.2 can be translated into a prediction for  $\cos \delta$  as [37]<sup>2</sup>

$$\cos \delta = \frac{\tan \theta_{23} \sin \theta_{12}^2 + \sin \theta_{13}^2 \cos \theta_{12}^2 / \tan \theta_{23} - (\sin \theta_{12}^\nu)^2 (\tan \theta_{23} + \sin \theta_{13}^2 / \tan \theta_{23})}{\sin 2\theta_{12} \sin \theta_{13}}, \quad (3.3)$$

where only the parameter  $\sin \theta_{12}^\nu$  is model dependent and we have respectively  $\sin \theta_{12}^\nu = 1/\sqrt{3}$ ,  $\sin \theta_{12}^\nu = 1/\sqrt{2}$ ,  $\tan \theta_{12}^\nu = 1/\varphi$  and  $\theta_{12}^\nu = \pi/5$ ,  $\cos \theta_{12}^\nu = \varphi/\sqrt{3}$  and  $\theta_{12}^\nu = \pi/6$  for mixing based on TB, BM, GRa, GRb, GRc and HEX where  $\varphi = (1 + \sqrt{5})/2$ .

Let us discuss an approximation of the sum rules for the TB mixing as an example, where  $\sin \theta_{12}^\nu = 1/\sqrt{3}$ . We can re-write Equation (3.3) using the parameters  $s$ ,  $a$  and  $r$  defined in Equation (2.16) and then expand in them. The linearised sum rule reads [34]

$$\cos \delta = \frac{s}{r}, \quad (3.4)$$

but it does not describe adequately the exact sum rules as shown in the left panel of Figure 4. Therefore we can go to the second order expansion, which is

$$\cos \delta = \frac{s}{r} + \frac{r^2 + 8as}{4r}, \quad (3.5)$$

<sup>2</sup>See also [38].

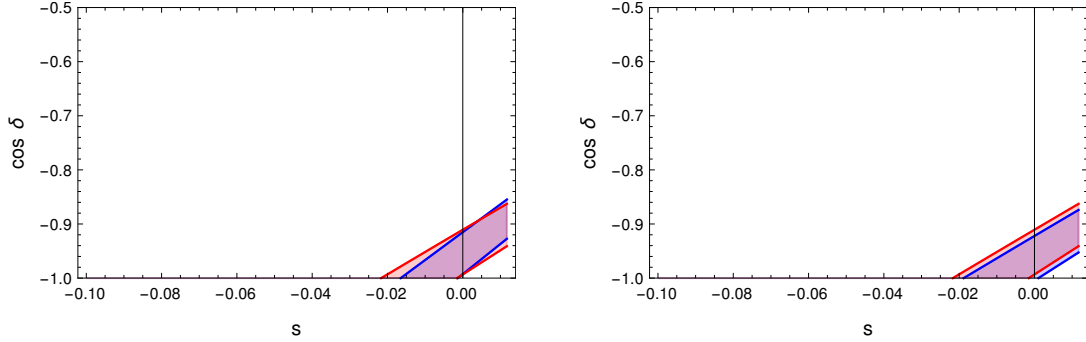


**Figure 5:** *Solar* mixing sum rule predictions for BM neutrino mixing. In the both panels the red band is the allowed region of the exact BM *solar* sum rules using the  $3\sigma$  range of  $r$  (i.e. the deviation of  $\sin\theta_{13}$ ) and it is plotted in the  $3\sigma$  range of  $s$  (i.e. the deviation of  $\sin\theta_{23}$  from the TB value) and using the value  $a = -0.1$ . The blue band is given by the linearised sum rule in the left panel. In the right panel the blue band is the second order expansion sum rule prediction, it matches the exact sum rule.

and it matches the exact sum rule behaviour as seen on the right panel in Figure 4. Similarly we can obtain higher order expansion for the other cases and check them against the data, like for the BM case showed in Figure 5. In this case we did not choose the best fit value for  $a$  because otherwise it would fall out of the physical range of  $\cos\delta$  since BM is almost excluded by the data. The approximated expression for the sum rules can help us understand its behaviour and the dependence of  $\cos\delta$  on the other parameters that are in general non-linear and assess the deviation from the non-corrected PMNS mixing. We then expect for the exact sum rules a first order linear dependence on  $s$ .

In Figure 6 we present the exact sum rules prediction from Equation (3.3) for TB, BM, GRa, GRb, GRc and HEX and the constraints from the fit of the neutrino oscillation data [31]. We require  $\cos\delta$  to fall in the physical range  $-1 < \cos\delta < 1$  and we present it in the y-axis. In all panel the x-axis is  $\sin^2\theta_{12}$  and the different colour bands are sampled in the allowed  $\sin\theta_{23}$  region. The width of the band is given by allowing  $\sin\theta_{13}$  to vary in its  $3\sigma$  range. We notice that the  $\theta'_{12} = 45^\circ$  BM mixing (top-right panel) is closed to be excluded at  $3\sigma$  and only low values of  $\sin^2\theta_{12}$  and high values of  $\sin^2\theta_{12}$  are still viable. Similarly for GRc mixing (bottom-left panel), with  $\cos\theta'_{12} = \varphi/3$ , the viable parameter space is very tight, only for maximal values of  $\sin\theta_{13}$  and minimal values of  $\sin\theta_{12}$  and  $\sin\theta_{23}$  we can obtain physical results for the CP phase. For TB mixing (top-left panel) with  $\sin\theta'_{12} = 1/\sqrt{3}$  in the neutrino sector with charged lepton correction lead consistent results in all parameters space, with the prediction for  $\cos\delta$  that shows an approximately linear dependence on  $\sin^2\theta_{12}$  as understood by the leading order term in the sum rules in Equation (3.4). The prediction for the CP phase lies in the  $0.52 \lesssim \cos\delta \lesssim 0.12$  range. The yellow and green bands are the  $1\sigma$  range respectively of  $\sin^2\theta_{12}$  and  $\cos\delta$  and we notice how these ranges favor GRa and GRb mixing. For both these models we see that the prediction of  $\cos\delta$  are in the negative plane. For GRa (center-left panel), with  $\tan\theta'_{12} = 1/\varphi$ , the whole parameter space leads to physical prediction of  $\cos\delta$ . For GRb (center-right panel),

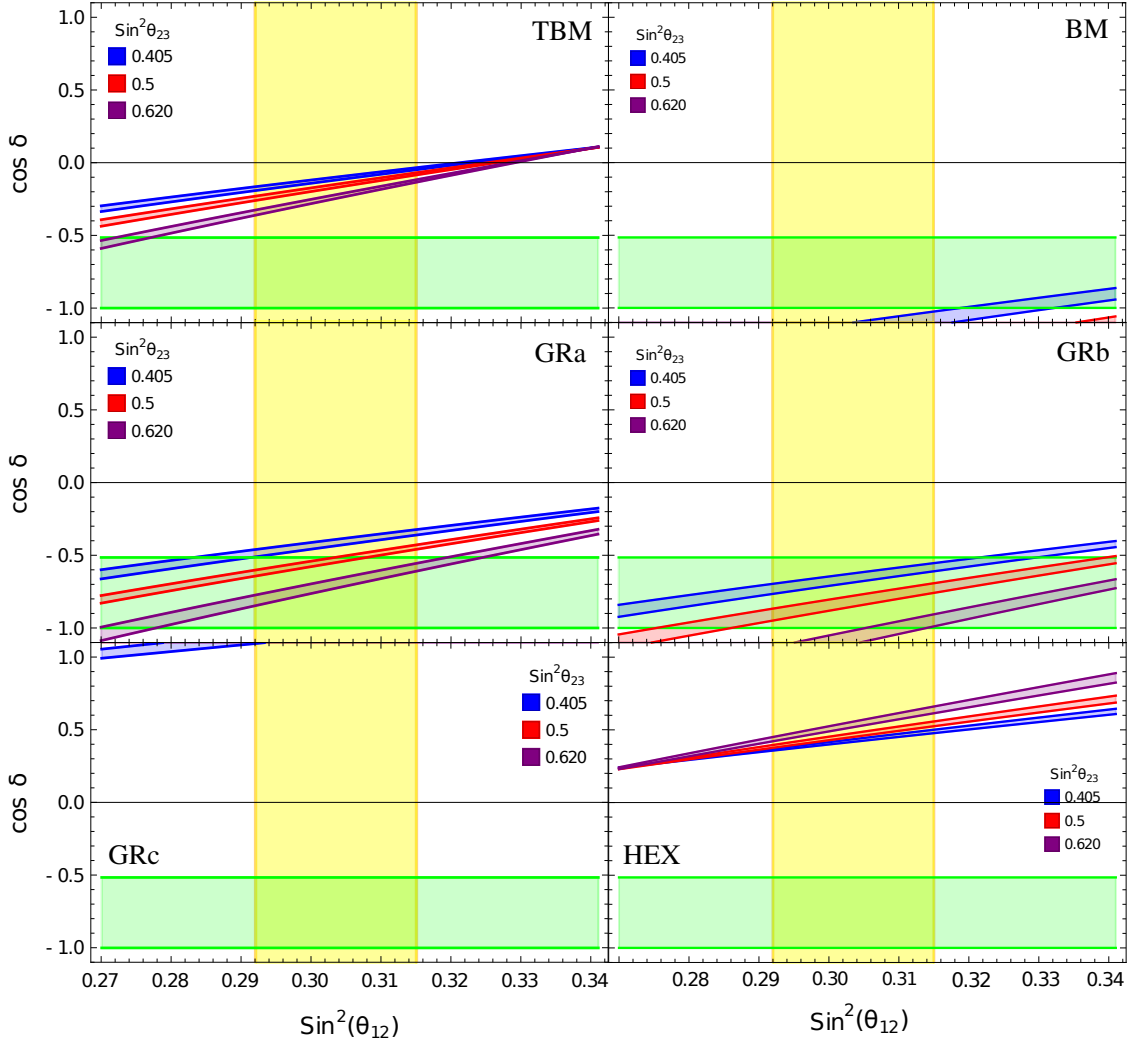


**Figure 6:** Summary of exact *solar* sum rule predictions for different types of neutrino mixing. In the top left hand panel we present with the different colored band the sum rule prediction for TB for  $\cos \delta$  letting  $\sin \theta_{12}$  vary in its  $3\sigma$  range, the different color denoted different choice of  $\sin \theta_{23}$  given in the legend, in its  $3\sigma$  range and the width of the band is given by the  $3\sigma$  range in  $\sin \theta_{13}$ . The green and yellow band are the  $1\sigma$  range for respectively  $\cos \delta$  and  $\sin \theta_{23}$ . Similar plots for BM, GRa, GRb, GRc and HEX are presented respectively on the top right, center right, center left, bottom left, bottom right panels.

with  $\theta_{12}' = \pi/5$  mixing, larger values  $\sin \theta_{23}$  are excluded for small values of  $\sin^2 \theta_{12}$ . We finally notice that TM and HEX are the only model predicting positive values of  $\cos \delta$  and HEX (bottom-right panel), with  $\theta_{12}' = \pi/6$  in particular the only predicting values of  $\cos \delta \gtrsim 0.2$ . Of the mixing pattern we studied GRa and GRb are favoured by the current  $1\sigma$  ranges and BM and GRc are much disfavoured and only consistent with the far corners of the parameter space with a prediction of  $|\cos \delta| \approx 1$ .

## 4 Atmospheric sum rules

In this section we discuss the second possibility, that is to have the T generator unbroken, therefore the charged lepton mixing matrix is exactly diagonal. In this case the correction to the PMNS matrix predicted from the group  $G$  comes from the neutrino sector and it provides a non zero reactor angle. For each group there are two possible corrections achieved either breaking U and preserving S or with S and U broken and SU preserved. Therefore for each discrete symmetry we will study two mixing pattern [39–41].

Let us consider again  $G = S_4$  and the TB mixing in Equation (1.3) as an example. If we break  $S$  and  $U$  but preserve  $SU$  the first column of the TB matrix is preserved and we have the so-called TM1 mixing pattern [42, 43]

$$U_{\text{TM1}} \approx \begin{pmatrix} \sqrt{\frac{2}{3}} & - & - \\ -\frac{1}{\sqrt{6}} & - & - \\ \frac{1}{\sqrt{6}} & - & - \end{pmatrix}, \quad (4.1)$$

if instead  $S$  is unbroken the second column is preserved and we have the second mixing pattern TM2

$$U_{\text{TM2}} \approx \begin{pmatrix} - & \sqrt{\frac{1}{3}} & - \\ - & \sqrt{\frac{1}{3}} & - \\ - & -\sqrt{\frac{1}{3}} & - \end{pmatrix}. \quad (4.2)$$

We can explicitly check this noticing that

$$S \begin{pmatrix} \sqrt{\frac{1}{3}} \\ \sqrt{\frac{1}{3}} \\ \sqrt{\frac{1}{3}} \end{pmatrix} = \begin{pmatrix} \sqrt{\frac{1}{3}} \\ \sqrt{\frac{1}{3}} \\ \sqrt{\frac{1}{3}} \end{pmatrix}, \quad (4.3)$$

meaning that the second column of the TB mixing matrix is an eigenvector of the S matrix. Similarly for the first column with the  $SU$  matrix. In this second case where the second column of TB matrix is conserved we have

$$|U_{e2}| = |U_{\mu 2}| = |U_{\tau 2}| = \frac{1}{\sqrt{3}}, \quad (4.4)$$

and given the parametrisation in Equation (2.6) we have

$$|U_{e2}| = |s_{12}c_{13}|, \quad |U_{\mu 2}| = |c_{12}c_{23} - s_{12}s_{13}s_{23}e^{i\delta}|, \quad (4.5)$$

$$|U_{\tau 2}| = |-c_{12}s_{23} - s_{12}s_{13}c_{23}e^{i\delta}|. \quad (4.6)$$

Using the first equation  $|U_{e2}| = |s_{12}c_{13}|$  we have the first *atmospheric* sum rule

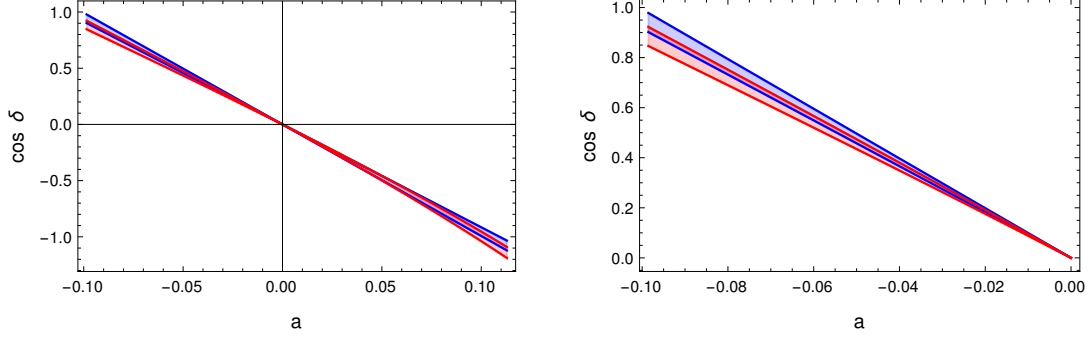


**Figure 7:** The red band is the allowed region of the exact TM2 sum rules using the  $3\sigma$  range of  $r$  (i.e. the deviation of  $\sin \theta_{13}$  and  $\sin \theta_{23}$  from the TB value). The red band is given by the linearised sum rule. On the right we zoom on the region  $-0.1 < a < 0$ .

$$s_{12}^2 = \frac{1}{3c_{13}^2}, \quad (4.7)$$

that allows us to write  $\theta_{12}$  in terms of  $\theta_{13}$  and removing a parameter in our description and gives a prediction that can be tested. Using Equation (4.7) and  $|c_{12}c_{23} - s_{12}s_{13}s_{23}e^{i\delta}|^2 = \frac{1}{3}$  we obtain the second *atmospheric* sum rule [42, 43]

$$\cos \delta = \frac{2c_{13} \cot 2\theta_{23} \cot 2\theta_{13}}{\sqrt{2 - 3s_{13}^2}}. \quad (4.8)$$

For the other models the discussion is similar where we call  $X_1$  and  $X_2$  the *atmospheric* sum rules respectively derived by preserving the first and second column of the unbroken group with mixing  $X$ . In terms of the deviation parameters for TM2 we have the sum rule

$$\cos \delta = \frac{2a(2+a)(-1+r^2)}{(1+a)\sqrt{1-2a-a^2r}\sqrt{4-3r^2}}. \quad (4.9)$$

We can expand this expression for small deviation parameters and at the zero-th order we have [39]

$$\cos \delta = -\frac{2a}{r} \quad (4.10)$$

and in Figure 7 we test this approximation against the exact sum rules using the experimental constraint in (2.9). We can see that given the updated data the linear approximation is now insufficient to describe the exact expression as it was instead in previous studies [39]. Similarly for TM1, as seen in Figure 8. This is true for the other model we will discuss later and therefore we provide the higher order expansions that agrees with the exact sum rule in Equation (4.9) given the current data and is

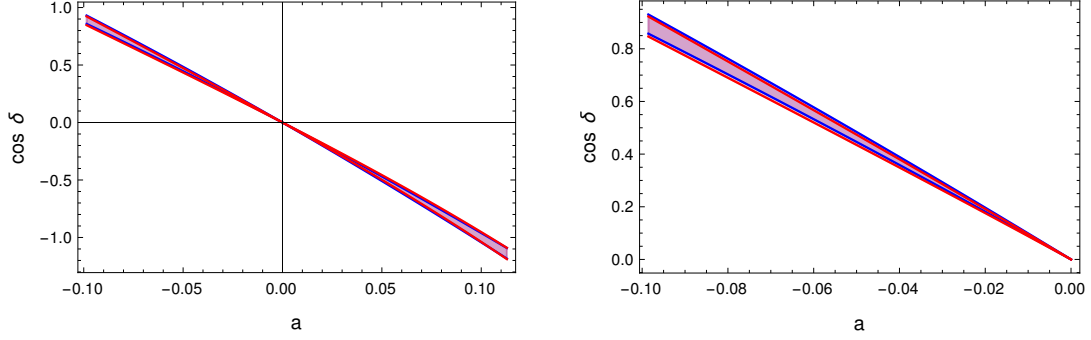


**Figure 8:** The red band is the allowed region of the exact TM2 sum rules using the  $3\sigma$  range of  $r$  (i.e. the deviation of  $\sin\theta_{13}$  and  $\sin\theta_{23}$  from the TB value). The blue band is given by the second order sum rule. On the right we zoom on the region  $-0.1 < a < 0$ .

$$\cos\delta = -\frac{2a}{r} - \frac{a^2}{r} \quad (4.11)$$

For the TM2 example we see in Figure 7 that the second order expansion is a good description of the exact sum rule. For TM1 instead, as shown in Figure 8 the third order expansion is needed. Since the second exact sum rules are quite involved having an

	Exact sum rule	Approximated sum rule
TM1	$\cos\delta = -\frac{\cot 2\theta_{23}(1-5\sin^2\theta_{13})}{2\sqrt{2}\sin\theta_{13}\sqrt{1-3\sin^2\theta_{13}}}$	$\cos\delta = \frac{a}{r} + \frac{a^2}{2r} + \frac{2a^3}{r} - \frac{7ar}{4}$
TM2	$\cos\delta = \frac{2\cos\theta_{13}\cot 2\theta_{23}\cot 2\theta_{13}}{\sqrt{2-3\sin^2\theta_{13}}}$	$\cos\delta = -\frac{2a}{r} - \frac{a^2}{r}$
GRa2	$\cos\delta = \frac{(1-\tan^2\theta_{23})\csc\theta(1-3\sin^2\theta_{13}+(1+\sin^2\theta_{13})\cos 2\theta)}{8\sin\theta_{13}\cos\theta_{23}\sqrt{\cos^2\theta_{13}-\sin^2\theta}}$	$\cos\delta = a\frac{\sqrt{1+\cos 2\theta}\csc\theta}{r}\left(1+\frac{a}{2}\right)$

**Table 1:** Exact and approximated sum rules for the experimentally viable models, where  $\theta = \arctan\frac{1}{\phi}$  and  $\phi = \frac{1+\sqrt{5}}{2}$ .

approximated expression is of help to understand the physical meaning of it and to understand the difference with respect to the TB model. We present in Table 1 the exact and approximated second sum rule for TM1, TM2 and GRa2 that as we will see later are the viable atmospheric mixing. Note that the approximated lead to simple results for TM1 and TM2 because the parameters  $a$ ,  $r$  and  $s$  are built as deviation parameters from the TB mixing and beyond the first order expansion may not bring new insight for other mixing. We present in Table 2 the first *atmospheric* sum rules used in Figure 9. These results were derived using the normal ordered data without SK atmospheric results, the discussion regarding linearisation is the same including SK or considering the inverted ordering since  $\sin\theta_{13}$  is very constrained and it does not change much in the different case considered.

TM1	$\cos \theta_{12} = \sqrt{\frac{2}{3}} \frac{1}{\cos \theta_{13}}$	TM2	$\sin \theta_{12} = \frac{1}{\sqrt{3} \cos \theta_{13}}$
BM1	$\cos \theta_{12} = \frac{1}{\sqrt{2} \cos \theta_{13}}$	BM2	$\cos \theta_{12} = \frac{1}{\sqrt{2} \cos \theta_{13}}$
GRa1	$\cos \theta_{12} = \frac{\cos \theta}{\cos \theta_{13}}$	GRa2	$\cos \theta_{12} = \frac{\sin \theta}{\cos \theta_{13}}$
GRb1	$\cos \theta_{12} = \frac{1+\sqrt{5}}{4 \cos \theta_{13}}$	GRb2	$\sin \theta_{12} = \frac{\sqrt{5+\sqrt{5}}}{4 \cos \theta_{13}}$
GRc1	$\cos \theta_{12} = \frac{1+\sqrt{5}}{2\sqrt{3} \cos \theta_{13}}$	GRc2	$\sin \theta_{12} = \frac{1+\sqrt{5}}{2\sqrt{3} \cos \theta_{13}}$
HEX1	$\cos \theta_{12} = \frac{\sqrt{3}}{2 \cos \theta_{13}}$	HEX2	$\sin \theta_{12} = \frac{1}{2\sqrt{2} \cos \theta_{13}}$

**Table 2:** Exact sum rules plotted in Figure 9. where  $\theta = \arctan \frac{1}{\phi}$  and  $\phi = \frac{1+\sqrt{5}}{2}$ .

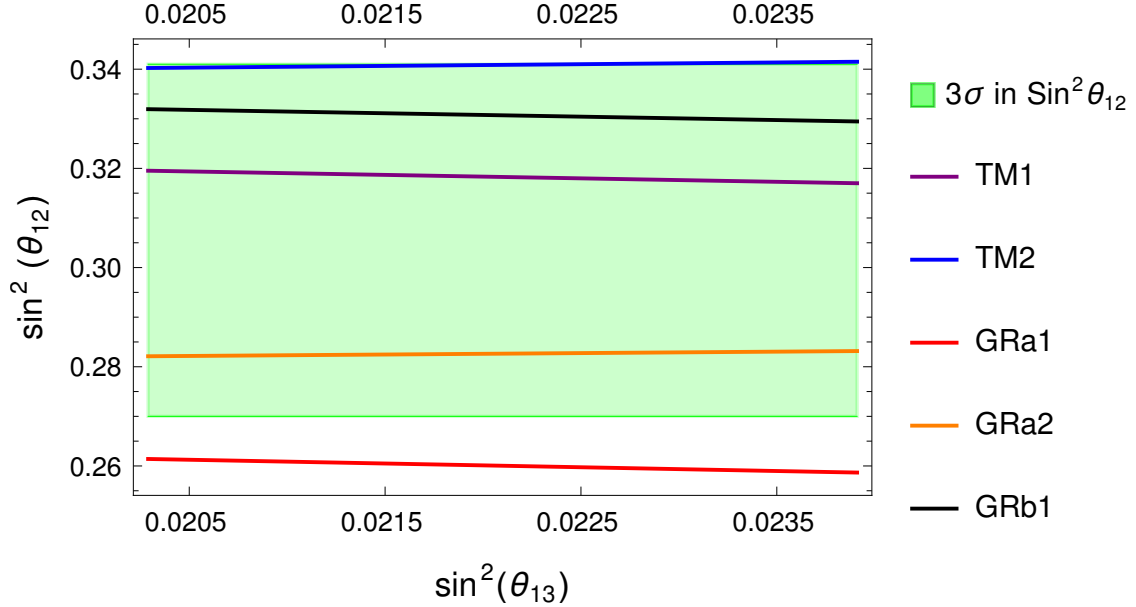


**Figure 9:** We present the  $3\sigma$  allowed region in green. The pink, blue, red, orange and black curves are respectively the predictions for TM1, TM2, GRa1, GRa2 and GRb1 mixing patterns.

In Figures 9 and 10 we study the exact *atmospheric* sum rules for models obtained modifying TB, BM, GRa, GRb, GRc and HEX. In Figure 9 we present first *atmospheric* sum rule in Table 2, where the green band is the  $3\sigma$  range for  $\sin^2 \theta_{12}$ . The models that do not appear are already excluded and far from the  $3\sigma$  region. Therefore BM1, BM2, GRa1, GRb2, GRc1, GRc2, HEX1 and HEX2 are already excluded. In red we show GRa1 that is excluded a  $3\sigma$  and in blue TM2, that is still not excluded only in a narrow parameter space, for high values of the solar and atmospheric angle. TM1 is showed in purple, GRa2



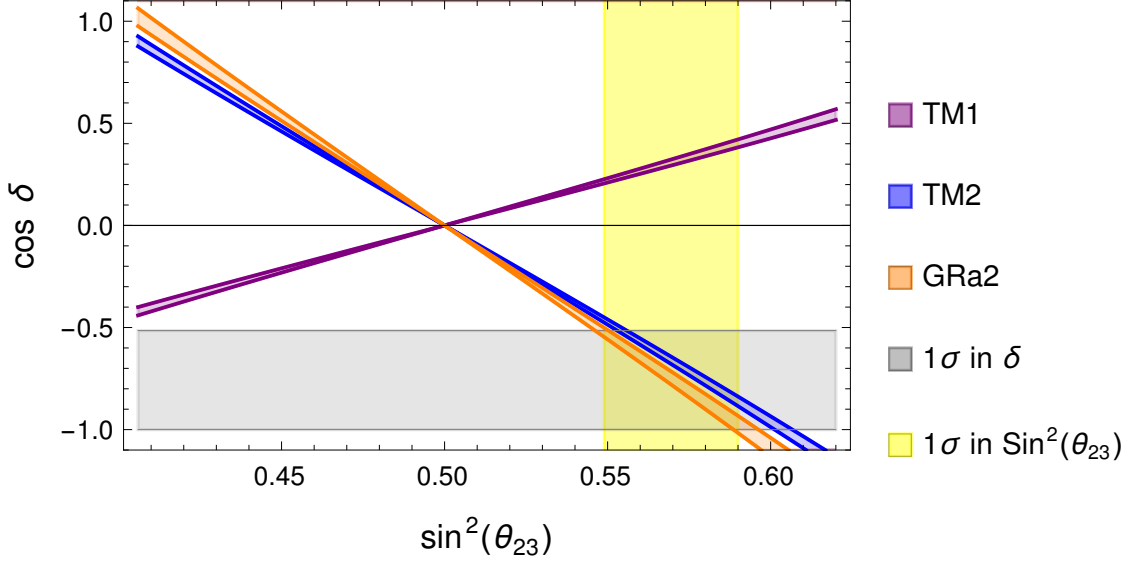


**Figure 10:** We present with the blue band the sum rule prediction for TM2 for  $\cos \delta$  letting  $\sin \theta_{13}$  vary in its  $3\sigma$  range. In orange and purple the sum rules for GRa2 and TM1. The yellow and gray regions are respectively the  $1\sigma$  range of  $\sin^2 \theta_{23}$  and  $\cos \delta$ , while the plot covers the whole  $3\sigma$  range.

in orange and GRb1 in black.

In Figure 10 we show the exact *atmospheric* sum rules (Table 1) and the corresponding equations for other models that are still allowed from Figure 9. We plot  $\cos \delta$  against  $\sin^2 \theta_{23}$  and letting  $\sin \theta_{13}$  vary in its  $3\sigma$  range, this gives the width of the different bands, in yellow and gray respectively are the  $1\sigma$  band for  $\sin^2 \theta_{23}$  and  $\cos \delta$ . The GRb1 mixing do not appear in the plot because it lays in unphysical values of  $\cos \delta$ . In purple, blue and orange we present TM1, TM2 and GR12. We can see that given the  $1\sigma$  bands, the GRa2 mixing is favoured when considering normal ordering and without the SK data, since TM2 is allowed only on a small portion of the parameter space as shown in Figure 9.

## 5 Littlest Seesaw

The Littlest Seesaw (LS) mechanism is the most economic neutrino mass generation mechanism that is still consistent with the experimental neutrino data [18, 19]. We will show that after the choice of a specific  $n$  value, all the neutrino observables are fixed by two free parameters. Different values of  $n$  can be realised by different discrete symmetry groups. The LS introduces two new Majorana right-handed (RH) neutrinos  $N_R^{atm}$  and  $N_R^{sol}$  that will be mostly responsible for providing the atmospheric and solar neutrino mass respectively and the lightest SM neutrino is approximately massless; this is the idea of sequential dominance (SD) of RH neutrinos combined with the requirement for the  $N_R^{atm} - \nu_e$  interaction to be zero [44]. The Majorana neutrino mass matrix is given by the standard type I seesaw equation

$$m^\nu = -m^D M_R^{-1} m^{D^T}, \quad (5.1)$$

where the RH neutrino mass matrix  $M_R$  is a  $2 \times 2$  diagonal matrix

$$M_R = \begin{pmatrix} M_{\text{atm}} & 0 \\ 0 & M_{\text{sol}} \end{pmatrix}, \quad M_R^{-1} = \begin{pmatrix} M_{\text{atm}}^{-1} & 0 \\ 0 & M_{\text{sol}}^{-1} \end{pmatrix}, \quad (5.2)$$

that comes from the Lagrangian term

$$\mathcal{L}_{\text{LS}} \supset -\frac{1}{2} M_{\text{atm}} \bar{N}_R^{\text{atm}} N_R^{\text{atm}} - \frac{1}{2} M_{\text{sol}} \bar{N}_R^{\text{sol}} N_R^{\text{sol}} + h.c. . \quad (5.3)$$

The Dirac mass matrix is instead a  $3 \times 2$  matrix with arbitrary entries

$$m^D = \begin{pmatrix} d & a \\ e & b \\ f & c \end{pmatrix}, \quad (m^D)^T = \begin{pmatrix} d & e & f \\ a & b & c \end{pmatrix}, \quad (5.4)$$

where the entries are the coupling between the Majorana RH neutrinos and the SM neutrinos. The first column describe the interaction of the neutrinos in the flavour basis with the atmospheric RH neutrino and the second with the solar RH neutrino. The SD assumptions are that  $d = 0$ ,  $d \ll e, f$ , and

$$\frac{(e, f)^2}{M_{\text{atm}}} \gg \frac{(a, b, c)^2}{M_{\text{sol}}}, \quad (5.5)$$

these, together with the choice that of the almost massless neutrino to be the first mass eigenstate  $m_1$ , leads to  $m_3 \gg m_2$  and therefore a normal mass hierarchy. This description can be further constrained choosing exactly  $e = f$ ,  $b = na$  and  $c = (n - 2)a$  giving a simplified Dirac matrix

$$m^D = \begin{pmatrix} 0 & a \\ e & na \\ e & (n - 2)a \end{pmatrix}, \quad (5.6)$$

that is called constrained dominance sequence (CSD) for positive integer  $n$  [9, 17, 18]. Following the literature we will refer to models with  $n$  real as LS models [19]. It has been shown that the reactor angle is [19]

$$\theta_{13} \sim (n - 1) \frac{\sqrt{2} m_2}{3 m_3}, \quad (5.7)$$

therefore this can provide non-zero and positive angle for  $n > 1$  and also excludes already models with  $n \geq 5$  since they do not fit the experimental value.

The littlest seesaw Lagrangian unifies in one triplet of flavour symmetry the three families of electroweak lepton doublets while the two extra right-handed neutrinos,  $\nu_R^{\text{atm}}$  and  $\nu_R^{\text{sol}}$  are singlets and reads [19]

$$\mathcal{L} = -y_{\text{atm}} \bar{L} \cdot \phi_{\text{atm}} \nu_R^{\text{atm}} - y_{\text{sol}} \bar{L} \cdot \phi_{\text{sol}} \nu_R^{\text{sol}} - \frac{1}{2} M_{\text{atm}} \nu_R^{\text{atm}} \bar{\nu}_R^{\text{atm}} - \frac{1}{2} M_{\text{sol}} \nu_R^{\text{sol}} \bar{\nu}_R^{\text{sol}} + h.c. , \quad (5.8)$$

which can be enforced by a  $Z_3$  symmetry and where  $\phi_{\text{atm}}$  and  $\phi_{\text{sol}}$  can be either Higgs-like triplets under the flavour symmetry or a combination of Higgses electroweak doublets and flavons depending on the specific choice of symmetry to use. In both cases the alignment should follow

$$\phi_{\text{atm}}^T \propto (0, 1, 1), \quad \phi_{\text{sol}}^T \propto (1, n, n - 2), \quad (5.9)$$

or

$$\phi_{\text{atm}}^T \propto (0, 1, 1), \quad \phi_{\text{sol}}^T \propto (1, n - 2, n). \quad (5.10)$$

We will refer to the first possibility in Equation (5.9) as the normal case and the second, in Equation (5.10) as the flipped case. The predictions for  $n$  in the flipped case are related to the normal one, as we will discuss later, by

$$\tan \theta_{23} \rightarrow \cot \theta_{23} \quad \delta \rightarrow \delta + \pi, \quad (5.11)$$

therefore we will discuss them together as one single  $n$  case.

There is an equivalent convention that can be found in the literature [29], where the alignment is chosen to be

$$\phi_{\text{atm}}^T \propto (0, 1, -1), \quad \phi_{\text{sol}}^T \propto (1, n, 2 - n). \quad (5.12)$$

or

$$\phi_{\text{atm}}^T \propto (0, 1, -1), \quad \phi_{\text{sol}}^T \propto (1, 2 - n, n). \quad (5.13)$$

that leads to the same results as the previous two cases respectively. In the neutrino mass matrix there will appear a  $(-1)$  factor that is only a non-physical phase that can therefore be neglected. In particular the case  $n = 1 + \sqrt{6}$  that can be obtained with modular symmetry in [29] is still  $n = 1 + \sqrt{6}$  in our convention using the Equation (5.9).

We will compute everything following the derivation in [19] and using Equation (5.9) and deriving the flipped result with Equation (5.11). We will consider  $n = 2.5, 3$  and

$1 + \sqrt{6} \approx 3.45$  and their flipped cases. The mass matrix then in the diagonal charged lepton basis is given by

$$m^\nu = m_a \begin{pmatrix} 0 & 0 & 0 \\ 0 & 1 & 1 \\ 0 & 1 & 1 \end{pmatrix} + m_b e^{i\eta} \begin{pmatrix} 1 & n & n-2 \\ n & n^2 & n(n-2) \\ 1 & n(n-2) & (n-2)^2 \end{pmatrix}, \quad (5.14)$$

where we used Equations (5.1), (5.2) and (5.6)

$$m_a = \frac{|e|^2}{M_{\text{atm}}} \quad m_b = \frac{|a|^2}{M_{\text{sol}}}, \quad (5.15)$$

and the only relevant phase is  $\eta = \arg(a/e)$ . At this point we notice that, in the diagonal charged lepton mass basis where we work, the PMNS mixing matrix is fully specified by the choice of  $n$  and the parameters  $m_a/m_b$  and  $\eta$ . Indeed it is possible to derive exact analytic results for the masses and mixing angles [19], and hence obtain the LS prediction for the neutrino oscillation observables.

We first observe that

$$m^\nu \begin{pmatrix} \sqrt{\frac{2}{3}} \\ -\sqrt{\frac{1}{3}} \\ \sqrt{\frac{1}{3}} \end{pmatrix} = \begin{pmatrix} 0 \\ 0 \\ 0 \end{pmatrix}, \quad (5.16)$$

where the vector  $(\sqrt{\frac{2}{3}}, -\sqrt{\frac{1}{3}}, \sqrt{\frac{1}{3}})^T$  is the first column of the TB matrix in Equation (1.3) and is then an eigenvector of the neutrino mass matrix with eigenvalue 0 and it corresponds to the massless neutrino eigenstate. This means that for a generic  $n$  we get a TM1 mixing, Equation (4.1), where the first column of the TB matrix is preserved and the other two can change. Therefore we can think of the LS as a special case of the *atmospheric* sum rules for the TB mixing. Since the *atmospheric* sum rules were derived only using the fact that the first column of the TB matrix is preserved all LS implementations also follow the TM1 sum rules in Equation (4.1). Once we have noticed this it is clear that  $m_\nu$  can be block diagonalised using the TB matrix

$$m_{\text{block}}^\nu = U_{\text{TB}}^T m^\nu U_{\text{TB}} = \begin{pmatrix} 0 & 0 & 0 \\ 0 & x & y \\ 0 & y & z \end{pmatrix}, \quad (5.17)$$

with

$$x = 3m_b e^{i\eta}, \quad y = \sqrt{6}m_b e^{i\eta}(n-1), \quad z = |z|e^{i\phi_z} = 2[m_a + m_b e^{i\eta}(n-1)^2]. \quad (5.18)$$

Finally we diagonalise  $m_{\text{block}}^\nu$  to obtain a matrix  $\text{diag}(0, m_2, m_3)$

$$U_{\text{block}}^T m_{\text{block}}^\nu U_{\text{block}} = P_{3\nu}^* R_{23\nu}^T P_{2\nu}^* m_{\text{block}}^\nu P_{2\nu} P_{23\nu} P_{3\nu} = m_{\text{diag}}^\nu = \text{diag}(0, m_2, m_3), \quad (5.19)$$

where the phases are

$$P_{2\nu} = \begin{pmatrix} 1 & 0 & 0 \\ 0 & e^{i\phi_2^\nu} & 0 \\ 0 & 0 & e^{i\phi_3^\nu} \end{pmatrix}, \quad (5.20)$$

$$P_{3\nu} = \begin{pmatrix} e^{i\omega_1^\nu} & 0 & 0 \\ 0 & e^{i\omega_2^\nu} & 0 \\ 0 & 0 & e^{i\omega_3^\nu} \end{pmatrix},$$

and the angle we use to diagonalise

$$R_{23\nu} = \begin{pmatrix} 1 & 0 & 0 \\ 0 & \cos \theta_{23}^\nu & \sin \theta_{23}^\nu \\ 0 & -\sin \theta_{23}^\nu & \cos \theta_{23}^\nu \end{pmatrix} \equiv \begin{pmatrix} 1 & 0 & 0 \\ 0 & c_{23}^\nu & s_{23}^\nu \\ 0 & -s_{23}^\nu & c_{23}^\nu \end{pmatrix}, \quad (5.21)$$

with the angle being fully specified by the free parameters  $m_a/m_b$  and  $\eta$

$$t \equiv \tan 2\theta_{23}^\nu = \frac{2|y|}{|z| \cos(A - B) - |x| \cos B}, \quad (5.22)$$

where

$$\tan B = \tan(\phi_3^\nu - \phi_2^\nu) = \frac{|z| \sin A}{|x| + |z| \cos A}, \quad (5.23)$$

and

$$A = \phi_z - \eta = \arg [m_a + m_b e^{i\eta} (n-1)^2] - \eta. \quad (5.24)$$

The PMNS matrix is therefore the product of the TB and the  $U_{\text{block}}$  matrices

$$U_{\text{PMNS}} = U_{\text{block}}^T U_{\text{TB}}^T. \quad (5.25)$$

$$\sin \theta_{13} = \frac{1}{\sqrt{3}} s_{23}^\nu = \frac{1}{\sqrt{6}} \left( 1 - \sqrt{\frac{1}{1+t^2}} \right)^{1/2}$$

$$\tan \theta_{12} = \frac{1}{\sqrt{2}} c_{23}^\nu = \frac{1}{\sqrt{2}} (1 - 3 \sin^2 \theta_{13})^{1/2} \quad (5.26)$$

$$\tan \theta_{23} = \frac{\left| \frac{e^{iB}}{\sqrt{2}} c_{23}^\nu + \frac{1}{\sqrt{3}} s_{23}^\nu \right|}{\left| \frac{e^{iB}}{\sqrt{2}} c_{23}^\nu - \frac{1}{\sqrt{3}} s_{23}^\nu \right|} = \frac{|1 + \epsilon_{23}^\nu|}{|1 - \epsilon_{23}^\nu|},$$

with

$$\epsilon_{23}^\nu \equiv \sqrt{\frac{2}{3}} \tan \theta_{23}^\nu e^{-iB} = \sqrt{\frac{2}{3}} t^{-1} \left[ \sqrt{1+t^2} - 1 \right] e^{-iB}. \quad (5.27)$$

The neutrino masses can be computed from  $m_{\text{block}}^\nu$  and they are

$$H_{\text{block}}^\nu = m_{\text{block}}^\nu m_{\text{block}}^{\nu\dagger} = \begin{pmatrix} 0 & 0 & 0 \\ 0 & |x|^2 + |y|^2 & |x||y| + |y|e^{i\eta}z^* \\ 0 & |x||y| + |y|e^{-i\eta}z & |y|^2 + |z|^2 \end{pmatrix}, \quad (5.28)$$

and after diagonalisation we are left with

$$\begin{aligned} m_2^2 + m_3^2 &= T \equiv |x|^2 + 2|y|^2 + |z|^2, \\ m_2^2 m_3^2 &= D \equiv |x|^2 |z|^2 + |y|^4 - 2|x||y|^2 |z| \cos A, \end{aligned} \quad (5.29)$$

and finally

$$\begin{aligned} m_3^2 &= \frac{1}{2}T + \frac{1}{2}\sqrt{T^2 - 4D}, \\ m_2^2 &= D/m_3^2, \\ m_1^2 &= 0, \end{aligned} \quad (5.30)$$

and the CP phase is

$$\delta = -\arg \left( \text{sign}(t) e^{i\eta} \left( 4 \left( \sqrt{t^2 + 1} - 1 \right) + (-2 + 3e^{2iB}) t^2 \right) \right). \quad (5.31)$$

Therefore we notice that by just specifying two parameters, the phase  $\eta$  and the ratio of the masses  $r = m_a/m_b$  and choosing the  $n$  that eventually is determined by the choice of flavour symmetry, LS predicts all the neutrino oscillation observables, that is why it is called littlest seesaw.

Let us consider  $n = 3$  and the correspondent flipped case, which was realised successfully via  $S_4$  symmetry in [19]. We can plot the constraints on the parameter space given by the experimental ranges of  $\theta_{13}$  and the mass ratio  $m_2^2/m_3^2$ . In Figure 11 we notice that imposing these two experimental constraint leave only two small allowed parameter regions in the plane  $r - \eta$ . The allowed range we consider in  $r$  and  $\eta$  are given by the maximal and minimal values of them in the intersection of the blue and orange bands. Once we have the value of  $r$  and  $\eta$ , thanks to the high predictivity of the model we can derive all the physical parameters and we can test them against the observed values. We do this for different values of  $n$  in Table 3 to 5. We do not present the plot for the flipped case since it is exactly the same. In fact it involves only the mass ration and  $\theta_{13}$ . This fact

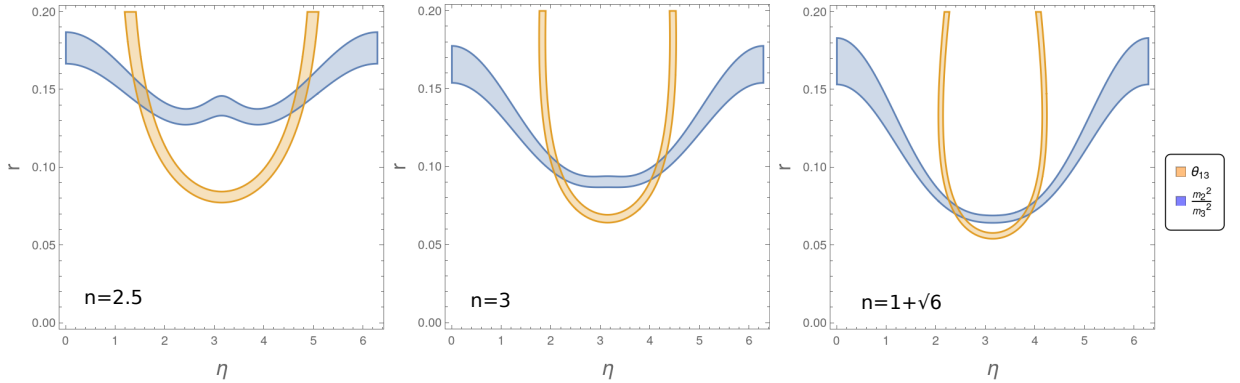


**Figure 11:** The parameters  $\eta$  and  $r$  are constrained to a good degree by only two experimental observables, namely  $\theta_{13}$  and the mass ratio  $m_2^2/m_3^2$ . The  $3\sigma$  allowed region for  $\theta_{13}$  and the mass ratio are respectively the orange and blue band. The area of intersection is the allowed parameter space for  $\eta$  and  $r$ . From the left to the right we present,  $n = 2.5$ , 3 and  $1 + \sqrt{6}$ .

	$n = 3$	$\eta = 2.1 \pm 0.3$	$\eta = 4.2 \pm 0.3$	Exp. range
	$\theta_{12} [^\circ]$	$34.3^{+0.4}_{-0.7}$	$34.3^{+0.4}_{-0.7}$	$31.27 - 35.86$
normal	$\theta_{23} [^\circ]$	$46^{+4}_{-5}$	$46^{+4}_{-5}$	$39.5 - 52.0$
normal	$\delta [^\circ]$	$93^{+12}_{-13}$	$255^{+12}_{-13}$	$0 - 45$ & $105 - 360$
flipped	$\theta_{23} [^\circ]$	$44^{+4}_{-5}$	$44^{+4}_{-5}$	$39.5 - 52.0$
flipped	$\delta [^\circ]$	$273^{+12}_{-13}$	$75^{+12}_{-13}$	$0 - 45$ & $105 - 360$

**Table 3:**  $3\sigma$  ranges of the predicted parameters and experimental ranges for  $n = 3$ . With  $r = 0.10 \pm 0.02$ .

can be understood easily studying the parameter  $t$  for example in the case  $n = 1 + \sqrt{6}$  and the flipped. In this case going from  $n$  to the flipped changes sign of  $t$  in Equation (5.22). The prediction for the mass ratio,  $\theta_{13}$ ,  $\theta_{12}$  are independent of this sign while  $\theta_{23}$  and  $\delta$  are affected by it, we can see this in Equations (5.26) and (5.31). The predictions as anticipated before are related by  $\tan \theta_{23} \rightarrow \cot \theta_{23}$  and  $\delta \rightarrow \delta + \pi$ .

In Table 3 we studied the  $n = 3$  and its flipped case. We present the theoretical prediction and its uncertainty coming from the allowed region in Figure 11 and the experimental bound. We notice that  $\eta = 2.1$  is still allowed only in the lower part of the  $\delta$  parameter space for the normal case and similarly  $\eta = 4.2$  for the flipped case. In Table 4 for  $n = 1 + \sqrt{6}$ , which can be realised with a modular symmetry [29], we notice that the region with  $\eta = 2.40$  is excluded thanks to the experimental bounds on  $\delta$  while the one with  $\eta = 3.88$  is well within the  $3\sigma$  range. For the flipped case instead  $\eta = 3.88$  is close the lower boundary of the  $3\sigma$  region in  $\delta$ . For  $n = 2.5$  in Table 5 we notice that  $\eta = 4.7$  is excluded for normal case while for the flipped both values are allowed in the  $3\sigma$  range. This case is also known in the literature as  $n = -1/2$  using the convention in Equation

	$n = 1 + \sqrt{6}$	$\eta = 2.40 \pm 0.04$	$\eta = 3.88 \pm 0.04$	Exp. range
	$\theta_{12} [^\circ]$	$34.4^{+0.4}_{-0.6}$	$34.4^{+0.4}_{-0.6}$	31.27 – 35.86
normal	$\theta_{23} [^\circ]$	$41.7^{+0.19}_{-0.12}$	$41.6^{+0.19}_{-0.12}$	39.5 – 52.0
normal	$\delta [^\circ]$	$75 \pm 3$	$285 \pm 3$	0 – 45 & 105 – 360
flipped	$\theta_{23} [^\circ]$	$48.3^{+0.19}_{-0.12}$	$48.4^{+0.19}_{-0.12}$	39.5 – 52.0
flipped	$\delta [^\circ]$	$255 \pm 3$	$103 \pm 3$	0 – 45 & 105 – 360

**Table 4:**  $3\sigma$  ranges of the predicted parameters and experimental ranges for  $n = 1 + \sqrt{6}$ . With  $r = 0.072 \pm 0.004$ .

(5.13). But it is more consistent to refer to it as  $n = 2.5$  in our notation. And in fact we notice that the LS that are still allowed by the data,  $n = 2.5$  and  $n = 1 + \sqrt{6}$  have  $n \sim 3$  which is the original CDS that worked.

	$n = 2.5$	$\eta = 1.5 \pm 0.4$	$\eta = 4.7 \pm 0.4$	Exp. range w/o SK
	$\theta_{12} [^\circ]$	$35.0 \pm 0.1$	$35.0 \pm 0.1$	31.27 – 35.86
normal	$\theta_{23} [^\circ]$	$47.0^{+3}_{-2}$	$46.5^{+4}_{-2}$	39.5 – 52.0
normal	$\delta [^\circ]$	$289 \pm 11$	$76 \pm 11$	0 – 45 & 105 – 360
flipped	$\theta_{23} [^\circ]$	$43.0^{+3}_{-2}$	$43.5^{+4}_{-2}$	39.5 – 52.0
flipped	$\delta [^\circ]$	$109 \pm 11$	$256 \pm 11$	0 – 45 & 105 – 360

**Table 5:**  $3\sigma$  ranges of the predicted parameters and experimental ranges for  $n = 2.5$ . With  $r = 0.15 \pm 0.02$ .

## 6 Conclusions

In the past decades many attempts have been made to explain the flavour structure of the PMNS matrix by imposing symmetry on the leptonic Lagrangian. These symmetries imply correlations among the parameters that are called sum rules. We have studied two types of sum rules: *solar* and *atmospheric* sum rules. The former breaks the  $T$  generator of a given symmetry group in the charged lepton sector in order to generate a non-zero reactor angle  $\theta_{13}$ . This leads with prediction for  $\cos \delta$  that can be tested against the experimental data. These in turn show a preference for GRa and GRb mixing while BM and GRc are constrained to live in a very small window of the parameter space.

The *atmospheric* sum rules instead come from either the breaking of both  $S$  and  $U$  in the neutrino sector while preserving  $SU$  or by breaking  $S$  and preserving  $U$ . In this case we have two relations among the parameters that can be tested. We noticed that only TM1, TM2 and GRa2 are still allowed by the neutrino oscillation data with a preference for GRa2 and with TM2 very close to be excluded.

We also studied LS models that follow the constrained sequential dominance idea with  $n$  allowed to be real. These models are very predictive with only two free real parameters



fixing all the neutrino oscillation observables. It is the most economical framework that explains the neutrino masses that is still compatible with data. Despite the great predictivity and the very small parameter space in the  $r - \eta$  plane allowed by the data all the LS examples we considered are still allowed in one part of the parameter space.

Finally, we note that the recent global fits to experimental data have provided significantly improved constraints on all of the above models and with future improvement in the neutrino oscillation data we will be able to restrict the pool of viable models still further. In particular advancements in the measurement of the leptonic CP violating Dirac phase  $\delta$  can strongly constrain more models in the near future. This is particularly true in LS models where already the experimental bounds on the CP phase is removing the degeneracy in the  $r - \eta$  parameter space and given the very precise theoretical prediction can strongly constrain these LS models. Future precision neutrino experiments are of great importance to continue to narrow down the possible PMNS flavour models and lead to a deeper understanding of this part of the flavour puzzle of the SM.

## Acknowledgments

The work is supported by the European Union Horizon 2020 Research and Innovation programme under Marie Skłodowska-Curie grant agreement HIDDeN European ITN project (H2020- MSCA-ITN-2019//860881-HIDDeN). SFK acknowledges the STFC Consolidated Grant ST/L000296/1.

## References

- [1] R. L. Workman *et al.* [Particle Data Group], PTEP **2022** (2022), 083C01 doi:10.1093/ptep/ptac097
- [2] A. Datta, F. S. Ling and P. Ramond, Nucl. Phys. B **671** (2003), 383-400 doi:10.1016/j.nuclphysb.2003.08.026 [arXiv:hep-ph/0306002 [hep-ph]].
- [3] W. Rodejohann, Phys. Lett. B **671** (2009), 267-271 doi:10.1016/j.physletb.2008.12.010 [arXiv:0810.5239 [hep-ph]].
- [4] S. Davidson and S. F. King, Phys. Lett. B **445** (1998), 191-198 doi:10.1016/S0370-2693(98)01442-7 [arXiv:hep-ph/9808296 [hep-ph]].
- [5] G. Altarelli, F. Feruglio and L. Merlo, JHEP **05** (2009), 020 doi:10.1088/1126-6708/2009/05/020 [arXiv:0903.1940 [hep-ph]].
- [6] D. Meloni, JHEP **10** (2011), 010 doi:10.1007/JHEP10(2011)010 [arXiv:1107.0221 [hep-ph]].
- [7] P. F. Harrison, D. H. Perkins and W. G. Scott, Phys. Lett. B **530** (2002), 167 doi:10.1016/S0370-2693(02)01336-9 [arXiv:hep-ph/0202074 [hep-ph]].
- [8] S. F. King and C. Luhn, Rept. Prog. Phys. **76** (2013), 056201 doi:10.1088/0034-4885/76/5/056201 [arXiv:1301.1340 [hep-ph]].
- [9] S. F. King, JHEP **08** (2005), 105 doi:10.1088/1126-6708/2005/08/105 [arXiv:hep-ph/0506297 [hep-ph]].
- [10] I. Masina, Phys. Lett. B **633** (2006), 134-140 doi:10.1016/j.physletb.2005.10.097 [arXiv:hep-ph/0508031 [hep-ph]].

- [11] S. Antusch and S. F. King, Phys. Lett. B **631** (2005), 42-47  
doi:10.1016/j.physletb.2005.09.075 [arXiv:hep-ph/0508044 [hep-ph]].
- [12] S. Antusch, P. Huber, S. F. King and T. Schwetz, JHEP **04** (2007), 060  
doi:10.1088/1126-6708/2007/04/060 [arXiv:hep-ph/0702286 [hep-ph]].
- [13] S. F. King, Phys. Lett. B **439** (1998), 350-356 doi:10.1016/S0370-2693(98)01055-7  
[arXiv:hep-ph/9806440 [hep-ph]].
- [14] S. F. King, Nucl. Phys. B **562** (1999), 57-77 doi:10.1016/S0550-3213(99)00542-8  
[arXiv:hep-ph/9904210 [hep-ph]].
- [15] S. F. King, Nucl. Phys. B **576** (2000), 85-105 doi:10.1016/S0550-3213(00)00109-7  
[arXiv:hep-ph/9912492 [hep-ph]].
- [16] P. H. Frampton, S. L. Glashow and T. Yanagida, Phys. Lett. B **548** (2002), 119-121  
doi:10.1016/S0370-2693(02)02853-8 [arXiv:hep-ph/0208157 [hep-ph]].
- [17] S. Antusch, S. F. King, C. Luhn and M. Spinrath, Nucl. Phys. B **856** (2012), 328-341  
doi:10.1016/j.nuclphysb.2011.11.009 [arXiv:1108.4278 [hep-ph]].
- [18] S. F. King, JHEP **07** (2013), 137 doi:10.1007/JHEP07(2013)137 [arXiv:1304.6264 [hep-ph]].
- [19] S. F. King, JHEP **02** (2016), 085 doi:10.1007/JHEP02(2016)085 [arXiv:1512.07531 [hep-ph]].
- [20] S. F. King and C. Luhn, JHEP **09** (2016), 023 doi:10.1007/JHEP09(2016)023  
[arXiv:1607.05276 [hep-ph]].
- [21] P. Ballett, S. F. King, S. Pascoli, N. W. Prouse and T. Wang, JHEP **03** (2017), 110  
doi:10.1007/JHEP03(2017)110 [arXiv:1612.01999 [hep-ph]].
- [22] S. F. King, S. Molina Sedgwick and S. J. Rowley, JHEP **10** (2018), 184  
doi:10.1007/JHEP10(2018)184 [arXiv:1808.01005 [hep-ph]].
- [23] S. F. King, Phys. Lett. B **724** (2013), 92-98 doi:10.1016/j.physletb.2013.06.013  
[arXiv:1305.4846 [hep-ph]].
- [24] S. F. King, JHEP **01** (2014), 119 doi:10.1007/JHEP01(2014)119 [arXiv:1311.3295 [hep-ph]].
- [25] F. Björkeröth and S. F. King, J. Phys. G **42** (2015) no.12, 125002  
doi:10.1088/0954-3899/42/12/125002 [arXiv:1412.6996 [hep-ph]].
- [26] P. T. Chen, G. J. Ding, S. F. King and C. C. Li, J. Phys. G **47** (2020) no.6, 065001  
doi:10.1088/1361-6471/ab7e8d [arXiv:1906.11414 [hep-ph]].
- [27] G. J. Ding, S. F. King, X. G. Liu and J. N. Lu, JHEP **12** (2019), 030  
doi:10.1007/JHEP12(2019)030 [arXiv:1910.03460 [hep-ph]].
- [28] G. J. Ding, S. F. King and C. Y. Yao, Phys. Rev. D **104** (2021) no.5, 055034  
doi:10.1103/PhysRevD.104.055034 [arXiv:2103.16311 [hep-ph]].
- [29] I. de Medeiros Varzielas, S. F. King and M. Levy, JHEP **02** (2023), 143  
doi:10.1007/JHEP02(2023)143 [arXiv:2211.00654 [hep-ph]].
- [30] F. J. de Anda and S. F. King, JHEP **06** (2023), 122 doi:10.1007/JHEP06(2023)122  
[arXiv:2304.05958 [hep-ph]].
- [31] I. Esteban, M. C. Gonzalez-Garcia, M. Maltoni, T. Schwetz and A. Zhou, JHEP **09** (2020),  
178 doi:10.1007/JHEP09(2020)178 [arXiv:2007.14792 [hep-ph]].

- [32] S. F. King and C. Luhn, *JHEP* **10** (2009), 093 doi:10.1088/1126-6708/2009/10/093 [arXiv:0908.1897 [hep-ph]].
- [33] G. Altarelli and F. Feruglio, *Nucl. Phys. B* **741** (2006), 215-235 doi:10.1016/j.nuclphysb.2006.02.015 [arXiv:hep-ph/0512103 [hep-ph]].
- [34] S. F. King, *Phys. Lett. B* **659** (2008), 244-251 doi:10.1016/j.physletb.2007.10.078 [arXiv:0710.0530 [hep-ph]].
- [35] S. F. King, *Phys. Lett. B* **718** (2012), 136-142 doi:10.1016/j.physletb.2012.10.028 [arXiv:1205.0506 [hep-ph]].
- [36] S. Antusch, K. Hinze and S. Saad, *JHEP* **08** (2022), 045 doi:10.1007/JHEP08(2022)045 [arXiv:2205.11531 [hep-ph]].
- [37] P. Ballett, S. F. King, C. Luhn, S. Pascoli and M. A. Schmidt, *JHEP* **12** (2014), 122 doi:10.1007/JHEP12(2014)122 [arXiv:1410.7573 [hep-ph]].
- [38] D. Marzocca, S. T. Petcov, A. Romanino, M. C. Sevilla, *JHEP* **1305** (2013) 073 [arXiv:1302.0423]; I. Girardi, S. T. Petcov, A. V. Titov, *Nucl. Phys. B* **894** (2015) 733 [arXiv:1410.8056 [hep-ph]]; S. T. Petcov, *Nucl. Phys. B* **892** (2015) 400 [arXiv:1405.6006 [hep-ph]]; J. Gehrlein, S. T. Petcov, M. Spinrath, A. V. Titov, *JHEP* **1611** (2016) 146 [arXiv:1608.08409 [hep-ph]]; I. Girardi, S. T. Petcov, A. V. Titov, *Nucl. Phys. B* **894** (2015) 733 [arXiv:1410.8056 [hep-ph]].
- [39] P. Ballett, S. F. King, C. Luhn, S. Pascoli and M. A. Schmidt, *Phys. Rev. D* **89** (2014) no.1, 016016 doi:10.1103/PhysRevD.89.016016 [arXiv:1308.4314 [hep-ph]].
- [40] D. Hernandez and A. Y. Smirnov, *Phys. Rev. D* **86** (2012), 053014 doi:10.1103/PhysRevD.86.053014 [arXiv:1204.0445 [hep-ph]].
- [41] C. Luhn, *Nucl. Phys. B* **875** (2013), 80-100 doi:10.1016/j.nuclphysb.2013.07.003 [arXiv:1306.2358 [hep-ph]].
- [42] C. H. Albright and W. Rodejohann, *Eur. Phys. J. C* **62** (2009), 599-608 doi:10.1140/epjc/s10052-009-1074-3 [arXiv:0812.0436 [hep-ph]].
- [43] C. H. Albright, A. Dueck and W. Rodejohann, *Eur. Phys. J. C* **70** (2010), 1099-1110 doi:10.1140/epjc/s10052-010-1492-2 [arXiv:1004.2798 [hep-ph]].
- [44] S. F. King, *JHEP* **09** (2002), 011 doi:10.1088/1126-6708/2002/09/011 [arXiv:hep-ph/0204360 [hep-ph]].